Heterogeneous Catalysis

International Edition: DOI: 10.1002/anie.201505452
German Edition: DOI: 10.1002/ange.201505452

Highly Dispersed SiO_x/Al_2O_3 Catalysts Illuminate the Reactivity of Isolated Silanol Sites

Aidan R. Mouat, Cassandra George, Takeshi Kobayashi, Marek Pruski, Richard P. van Duyne, Tobin J. Marks, and Peter C. Stair**

Abstract: *The reaction of γ-alumina with tetraethylorthosilicate (TEOS) vapor at low temperatures selectively yields monomeric SiO_x species on the alumina surface. These isolated $(\text{-AlO})_3Si(OH)$ sites are characterized by PXRD, XPS, DRIFTS of adsorbed NH_3, CO, and pyridine, and ^{29}Si and ^{27}Al DNP-enhanced solid-state NMR spectroscopy. The formation of isolated sites suggests that TEOS reacts preferentially at strong Lewis acid sites on the γ-Al_2O_3 surface, functionalizing the surface with "mild" Brønsted acid sites. For liquid-phase catalytic cyclohexanol dehydration, these SiO_x sites exhibit up to 3.5-fold higher specific activity than the parent alumina with identical selectivity.*

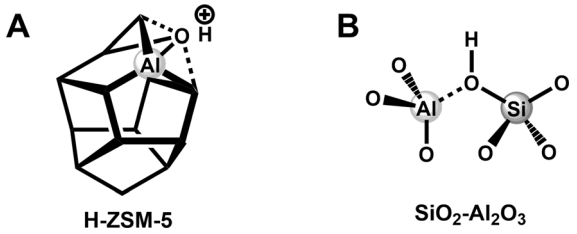

Figure 1. A) The pentasil unit of zeolite H-ZSM-5 with Al^{3+} substitution (all lattice points, except Al, represent Si atoms, with Si—O bonds omitted for clarity). B) A proposed Brønsted-acidic site in amorphous SiO_2–Al_2O_3.

Silica–aluminas are well-known solid acid catalysts and are employed in both laboratory organic synthesis and in large-scale industrial processes.[1] These materials include amorphous silica–aluminas, typically prepared by coprecipitation or sol–gel methods,[2] and ion-exchanged, crystalline aluminosilicate zeolites such as H-ZSM-5 or H-Y.[3] Solid acids catalyze a variety of transformations, including dehydration, skeletal isomerization, and cracking,[4] and are used in processes such as fluid catalytic cracking (FCC) and methanol-to-gasoline (MTG) synthesis.[5] In crystalline zeolites, "strong" Brønsted-acidic sites arise from isomorphous Al^{3+} substitution in the SiO_2 lattice, yielding "framework" protons as in Figure 1 a.[6] Amorphous silica–aluminas also possess Brønsted acid sites (Figure 1 b). Solid acids typically present a range of acid site strengths according to local coordination environments. Significant spectroscopic and physicochemical studies have been undertaken to characterize the strength and catalytic relevance of the different acid sites.[7]

In spite of advances in the synthesis and post-synthetic modification of solid acids, the non-uniformity of acid site strengths on solid acid catalysts remains a challenge. This non-uniformity can significantly compromise selectivity, leading to unwanted side products and ultimate deactivation by coking.[8] The attraction of tuning solid acid strength has been demonstrated in several organic transformations,[9] including recent work by Gazit and Katz[10] who reported the efficacy of mildly acidic silanol groups in β-glucan hydrolysis.[10] In recent work, van Bokhoven and co-workers demonstrated a controlled process for the synthesis of SiO_2–Al_2O_3 catalysts via chemical liquid deposition (CLD) grafting of Al and Si species on SiO_2 and Al_2O_3 supports.[7b,11] Here we report a new vapor phase approach to creating isolated, uniform, and weakly acidic SiO_x sites on alumina, and explore their catalytic properties with respect to a transformation of biomass relevance. Cyclohexanol dehydration is diagnostic of solid acid catalytic activity[12] and permits assessment of selectivity with respect to unwanted side reactions and coking, a traditional challenge to solid acid catalysis.[13]

We employ a strategy here that combines the mild conditions of a low temperature vapor-phase deposition process and the specific surface reactivity of γ-Al_2O_3 to realize a new class of SiO_x/Al_2O_3 catalysts featuring well-defined, isolated Si active sites having the structure $(\text{-AlO})_3Si(OH)$ (Scheme 1). These species are characterized by powder X-ray diffraction (PXRD), X-ray photoelectron spectroscopy (XPS), ^{29}Si and ^{27}Al solid-state NMR enhanced by dynamic

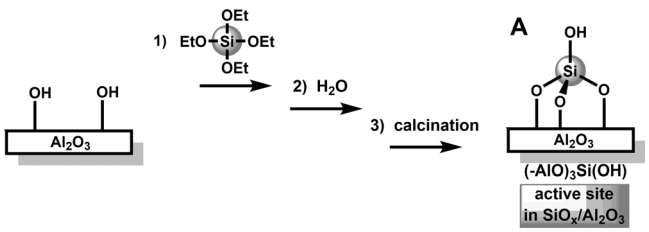

Scheme 1. Vapor-phase synthesis of $(\text{-AlO})_3Si(OH)$ sites on γ-Al_2O_3. Proposed active site in SiO_x/Al_2O_3 catalysts, **A**.

[*] A. R. Mouat, C. George, Prof. R. P. van Duyne, Prof. T. J. Marks, Prof. P. C. Stair
Chemistry Department and the Center for Catalysis and Surface Science, Northwestern University
2145 Sheridan Rd., Evanston, IL 60208 (USA)
E-mail: t-marks@northwestern.edu
pstair@northwestern.edu
Dr. T. Kobayashi, Prof. M. Pruski
U.S. DOE Ames Laboratory, and Department of Chemistry
Iowa State University
Ames, IA 50011 (USA)

Supporting information for this article is available on the WWW under http://dx.doi.org/10.1002/anie.201505452.

nuclear polarization (DNP), and diffuse reflectance infrared Fourier transform spectroscopy (DRIFTS) of adsorbed NH_3, CO, and pyridine, followed by catalytic studies. A linear relationship is demonstrated between the Si site density and surface Brønsted acidity. We also show that these SiO_x/Al_2O_3 catalysts are competent for the catalytic dehydration of cyclohexanol to cyclohexene, exhibiting up to 3.5-fold higher specific activity than the parent γ-Al_2O_3 with no loss in selectivity and with negligible coking.

Silica–alumina catalysts with multiple SiO_2 surface layers were previously prepared by chemical vapour deposition (CVD).[14] Atomic layer deposition (ALD) growth of SiO_2 on Si(100) wafers was achieved by George[15] using $SiCl_4 + H_2O$, while Ferguson obtained similar results using $Si(OEt)_4$ (TEOS) + H_2O.[16] Due to the low reactivity of SiO_2, an NH_3 co-feed was required in both cases to achieve efficient growth. However, Ma[17] reported that more nucleophilic Au/TiO_2 substrates nucleate SiO_2 growth using $Si(OMe)_4$ (TMOS) + H_2O without NH_3.

In the present strategy, SiO_x/Al_2O_3 catalysts are prepared at 50 °C by TEOS ALD on phase-pure γ-alumina (Alfa-Aesar, 60 m^2g^{-1}) in the viscous flow reactor described previously.[18] The ALD A-B type growth sequence (Figure S9; Supporting Information) is: 1) gaseous TEOS flow over the γ-Al_2O_3 for 120 s; 2) chamber purge for 240 s; 3) water vapor flow over the alumina for 300 s from a 25 °C reservoir; 4) chamber purge for 300 s (see Supporting Information for more details). After the ALD growth, the catalysts are calcined for 18 h at 550 °C in flowing O_2. Before deposition, no surface species other than C, Al, and O are detected on the alumina by XPS. The coverages of the deposited Si on the alumina (1.5–3.2 Si/nm^2) were assayed by inductively coupled plasma (ICP) analysis (Figure 2 A) with confirmation by XPS. Note here that the Si deposition saturates, independent of TEOS exposure time. Despite the A-B-type reaction sequence, substrate rehydroxylation does not result in further silica growth. Thus, the highest loading obtained is 3.2 Si/nm^2. Due to the low loading of Si, little change in Al surface character is observed spectroscopically (see below), as only a small fraction of surface sites are occupied by Si atoms. Brunauer–Emmett-Teller (BET) surface area analysis indicates constant surface area after ALD across all SiO_x loadings (Figure S9, representative isotherms in Figure S10), and scanning electron microscopy (SEM) evidences no obvious morphological changes, with the particle size remaining <3 μm by SEM (Figures S9 and S11). X-ray powder diffraction patterns of the catalysts remain unchanged after Si saturation, confirming the assignment of SiO_x as a surface species, neither intercalating into the γ-Al_2O_3 structure nor altering the catalyst crystallite size (Figure S12).

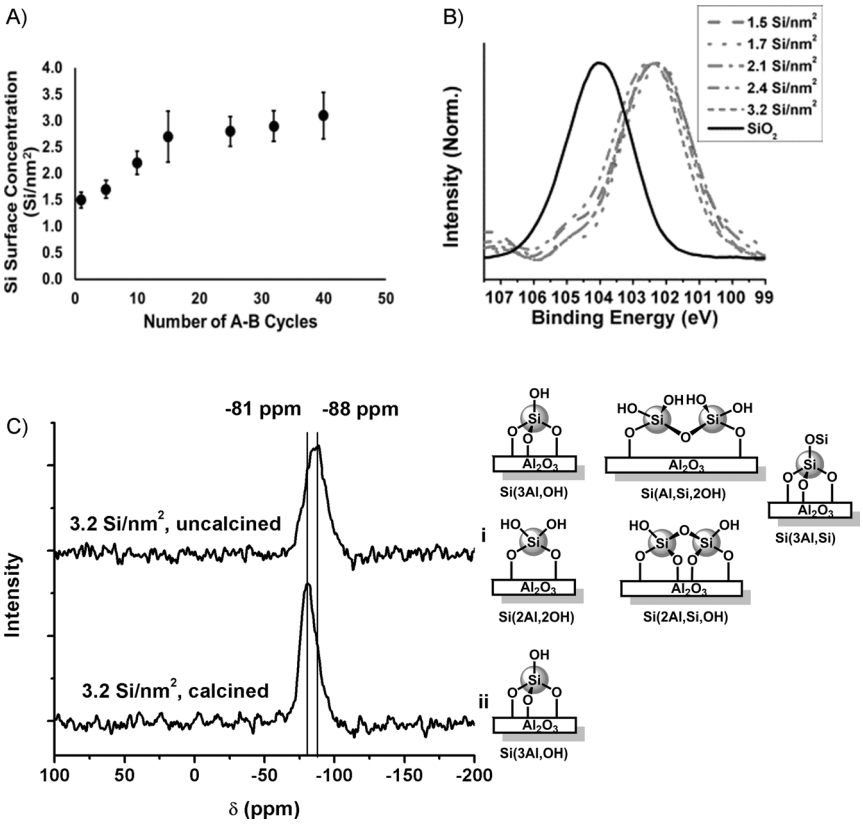

Figure 2. A) Si surface coverage in Si/nm^2 as determined by ICP. B) Si (2p) XPS spectrum of SiO_x catalysts. C) DNP-enhanced ^{29}Si CPMAS NMR spectra before and after calcining. Spectra were obtained at 100 K using MAS rate $\nu_R = 10$ kHz, recycle delay $\tau_{RD} = 1.5$ s, contact time $\tau_{CP} = 3$ ms, number of scans NS = 2048, acquisition time AT = 50 min. The surface structures Si(3Al,OH), Si(Al,Si,2OH), Si(2Al,2OH), Si(2Al,Si,OH), and Si(3Al,Si) are depicted on the right. Note that Si(3Al,OH) is the principle species in the calcined sample.

Next, an alternative growth mode in which all TEOS pulses were performed in sequence, followed by H_2O pulses, was investigated to determine if Si saturation occurs without A-B-cycling. While Si growth is again observed in this procedure, coverages reach only ca. 60 % of those observed for comparable numbers of A-B growth cycles. We speculate that deposition is sterically hindered by the presence of surface EtOH groups, consistent with previous observations in ALD processes.[19]

The SiO_x/Al_2O_3 sites were next characterized by XPS. The adventitious C(1s) carbon peak is referenced here to a binding energy (BE) of 285.0 eV. A higher energy feature assignable to C–O species[20] is not detected, even in uncalcined catalysts. The absence of residual surface −OEt moieties is further corroborated by solid-state NMR spectroscopy (see below). The Al(2p) BE occurs at 74.4 ± 0.2 eV for all catalysts after calcination, while the Al(2p) BE of reference γ-Al_2O_3 is found at 74.4 eV. Representative Al XPS spectra are shown in the Supporting Information (Figures S15–S17). The Si(2p) BE of the calcined SiO_x/Al_2O_3 sites is found at 102.4 ± 0.2 eV for all Si loadings (Figure 2 B) and differs from that of bulk SiO_2,

found here at 104.1 eV, in agreement with the literature.[21] Lower Si BEs relative to bulk silica are observed in other aluminosilicates, and have been assigned to Si-O-M structures[22] where M ≠ Si. Increased acidity in the silanol proton is attributable to this electronic effect.

The surface geometry of the ALD-derived SiO_x/Al_2O_3 sites was next probed by DNP-enhanced $^{29}Si\{^1H\}$ cross-polarization magic angle spinning (CPMAS) NMR spectroscopy (Figure 2C, i–ii).[23] The DNP technique boosts the sensitivity of conventional CPMAS by ca. 2 orders of magnitude through excitation of the exogenously administered biradicals at their ESR resonance frequency and concomitant transfer of magnetization to the nuclear spins (due to the low Si loadings of these catalysts, conventional ^{29}Si CPMAS NMR gave no detectable signals even after 40000 scans). In the uncalcined materials, the spectrum is assignable to sites Si(2Al,Si,OH), Si(Al,Si,2OH) and Si(3Al,Si) species which are all expected at $\delta = -85$ to -90 ppm.[24] Contributions from other sites, such as Si(2Al,2OH) and Si(3Al,OH), cannot be excluded a priori.[25] Furthermore, surface ethoxy groups cannot be detected by DNP-enhanced $^{13}C\{^1H\}$ CPMAS NMR (Figure S13), arguing that hydrolysis is essentially complete under the growth conditions.

The NMR results indicate that calcination enhances the Si site homogeneity and increases the density of Si-O-Al linkages, evidenced by narrowing and downfield displacement of the ^{29}Si signal. Moreover the $\delta = -81$ ppm position suggests that the major Si surface species after calcination has an Si(3Al,OH) geometry (Figure 2C, ii).[25b] Minor responses from the other species noted above are in principle possible; however, the spectroscopic and catalytic data (see below) argue that their contributions are minimal. Signals characteristic of Si(4Si) (ca. $\delta = -110$ ppm) and Si(3Si,OH) (ca. $\delta = -100$ ppm) sites[24] are also negligible, demonstrating, in agreement with the XPS data, that the Si deposition is limited by surface reactivity. Note that the present ^{29}Si NMR findings are consistent with other studies arguing that the final stable geometry of surface silica is a tridentate Si(3Al,OH) structure.[26] We speculate that here the geometry after calcination is a result of Si atom spatial isolation. Although the deposition process appears to yield some Si-O-Si linkages, polymeric SiO_2 does not form, so that during the 550 °C calcination, the Si surface atoms reconstruct in a final geometry dictated solely by the underlying γ-Al_2O_3 struture.

The DNP-enhanced $^{27}Al\{^1H\}$ CPMAS NMR measurements were carried out to selectively detect Al sites on the surface while excluding signals from underlying bulk Al_2O_3. The spectra of γ-Al_2O_3 and 3.2 Si/nm^2 SiO_x/Al_2O_3 before and after calcination (Figure S14) show two Al peaks assignable to octahedral sites (Al^{VI}, $\delta = 5$ ppm) and tetrahedral sites (Al^{IV}, $\delta = 65$ ppm).[24] Deposition of Si converts a fraction of Al^{VI} sites to Al^{IV} sites, with no peak shift or new signal apparent. The spectral intensities do not undergo any further change upon calcination, suggesting that the surface reconstruction by calcination involves primarily the Si species, a result corroborated by infrared spectroscopy (see below). Note that a small upfield shift (ca. 5 ppm) in the Al^{IV} peak is expected upon conversion of Al-OH to Al-O-Si bonds; however, due to the low Si loading only a small fraction of Al^{IV} sites have Al-O-Si bonds, precluding further interpretation of peak shape.

Ambient DRIFTS spectra of the catalysts were recorded at 100 °C after drying samples at 500 °C for 1 hour, using a KBr background (Figure S18). The spectral features are consistent with those previously noted in the literature.[27] Importantly, there is no shift in the position of the hydroxy signatures, hence no attenuation of the O–H bond strength, although there is lessened intensity of the bands at 3790 cm^{-1} and 3730 cm^{-1} similar to that previously reported for Si deposition on γ-Al_2O_3.[27b] This contrasts with the analogous but liquid-phase CLD process, which reveals attenuation under comparable conditions.[11a] Notable is the appearance of a sharp feature at 3723 cm^{-1} in the present SiO_x/Al_2O_3 catalyst, assignable to surface Si–OH species. Previously this peak was assigned at 3725–3745 cm^{-1},[27b,28] with the lower frequency mode associated with greater O–H bond ionicity, signifying enhanced Brønsted acidity. The 3723 cm^{-1} position is thus consistent with the present assignment of the Si-O-H sites as Brønsted acid sites.

NH_3 DRIFTS experiments were next conducted to probe surface acid sites, with catalyst surfaces exposed to NH_3 at 100 °C, then purged with Ar. The resulting spectra (Figure 3A,B) show that NH_3 interaction with the neat γ-alumina hydroxy groups gives rise to Al_n-OH···NH_3 features at 3769, 3727, and 3671 cm^{-1} (Figure 3A, i, ii) in agreement with the literature.[29] On ALD-derived SiO_x/Al_2O_3, an additional band at 3741 cm^{-1} (Figure 3A, iii, iv) is assigned to Si-OH···NH_3 species by analogy to similar modes in amorphous silica–aluminas.[8a,30] The acid-site DRIFTS spectral region

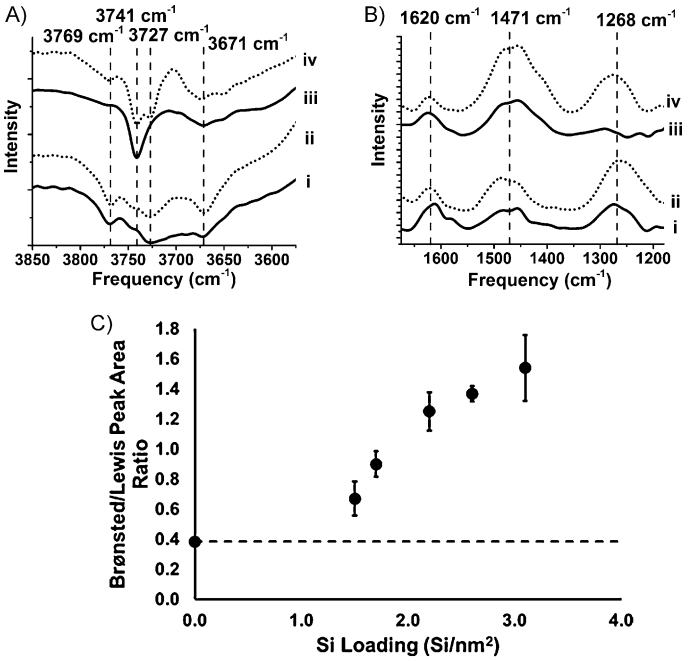

Figure 3. A) DRIFTS spectra of NH_3 treated SiO_x/Al_2O_3 for: i) uncalcined γ-Al_2O_3, ii) calcined γ-Al_2O_3, iii) uncalcined SiO_x/Al_2O_3 with 3.2 Si/nm^2, and iv) calcined SiO_x/Al_2O_3 with 3.2 Si/nm^2. B) DRIFTS acid region spectra of NH_3-treated SiO_x/Al_2O_3. C) Ratio of Brønsted-to-Lewis acid DRIFTS peak areas for NH_3 treated SiO_x/Al_2O_3 samples.

(Figure 3B, i–iv) shows three NH_3 bands on neat γ-Al_2O_3 at 1620, 1471, and 1268 cm^{-1}. Those at 1620 and 1268 cm^{-1} are assignable to NH_3 bound to weak and strong Al Lewis acid sites, respectively, while the feature at 1471 cm^{-1} is assigned to a Brønsted acid site-derived NH_4^+ mode.[31] In contrast, the DRIFTS spectrum of NH_3 on uncalcined SiO_x–Al_2O_3 exhibits only an Si–OH mode at 3741 cm^{-1} (Figure 3A, iii), indicating that the majority of the γ-Al_2O_3 hydroxy groups are consumed in the ALD process. While the band at 3769 cm^{-1} is usually associated with the most reactive Al-OH groups,[27a] here we find that all the alumina hydroxy groups react with gaseous TEOS. The SiO_x/Al_2O_3 DRIFTS acid region spectrum also indicates selective consumption of the strong Lewis acid sites related to the band at 1268 cm^{-1} (Figure 3B, iii), leaving the other acid sites unperturbed. It thus appears that the present ALD process involves coordination to, and presumably TEOS cleavage at, strong Lewis acid sites. When these sites are consumed, film growth ceases since the Si–OH units are insufficiently reactive to protonolyze the TEOS Si–OR linkage.

NH_3 adsorption on either uncalcined or calcined γ-Al_2O_3 reveals no obvous DRIFTS spectral differences (Figure 3A,B, i, ii). For NH_3 adsorportion on calcined Si-saturated SiO_x/Al_2O_3, similar Al–OH features at 3769, 3727, and 3671 cm^{-1} are visible (Figure 3A, , iv), however the Si–OH group signature at 3741 cm^{-1} remains strong, arguing that the Si species are not incorporated into the bulk γ-Al_2O_3. A strong Lewis acid peak at 1268 cm^{-1} is also evident (Figure 3B, iv) and resembles that of pure γ-Al_2O_3. The Brønsted acidity of the SiO_x/Al_2O_3 series was next assayed from the DRIFTS peak area ratio of Brønsted NH_4^+ to Lewis site···NH_3 species (Figure 3C). The linear correlation of this ratio with the Si surface density argues for enhanced Brønsted acidity of the new active sites. Additionally, the DRIFTS of adsorbed pyridine (Figure S20) confirms that there is no perturbation of the catalyst Lewis acid sites after Si deposition and calcination. DRIFTS of NH_3 spectra for individual catalyst loadings are shown in Figure S21.

CO DRIFTS was used to further probe surface hydroxy groups, since the O–H stretchinig frequency observed upon CO adsorption is sensitive to the Brønsted acidity, due to Al-OH···CO hydrogen-bonding.[32] At 100 °C, the DRIFTS spectrum of CO on pure γ-Al_2O_3 (Figure S19) reveals bands at 3794 and 3774 cm^{-1}, assignable to terminal tetrahedral and octahedral Al–OH groups, in excellent agreement with the literature.[33] ALD deposition of Si on the catalyst surface does not affect these peak positions, although a reduction in the 3794 cm^{-1} band intensity is noticable. A new OH band appears at 3726 cm^{-1} in the 3.2 Si/nm^2 catalyst spectrum, which is assigned here to isolated Si-OH groups on the basis of previous reports.[3b] Thus, the CO DRIFTS confirms the presence of isolated Si–OH sites, with no discernable attenuation of existing Al–OH groups.

The catalytic properties of the calcined SiO_x/Al_2O_3 materials were next evaluated for cyclohexanol dehydration in a batch reactor (see Figures S6 and S7 for details); catalytic data are compiled in Table S22, and summarized in Figure 4. It is seen that the present SiO_x/Al_2O_3 catalysts possess sufficiently strong Brønsted acid sites to catalyze this transformation but without formation of carbonaceous deposits typical of strong solid acids.[34] For ALD-derived SiO_x/Al_2O_3 catalysts, no products except cyclohexene are observed by GC-MS, and the carbon balance determined by an independent calibration of both cyclohexanol and cyclohexene is invariably 95–102 %. Since the cyclohexanol dehydration rate over SiO_x/Al_2O_3 exhibits a first-order dependence on [cyclohexanol], the rate constant k is determined from the slope of the cyclohexanol conversion versus time plot under differential conditions, i.e., when [cyclohexanol] is not significantly altered (Figure S22).

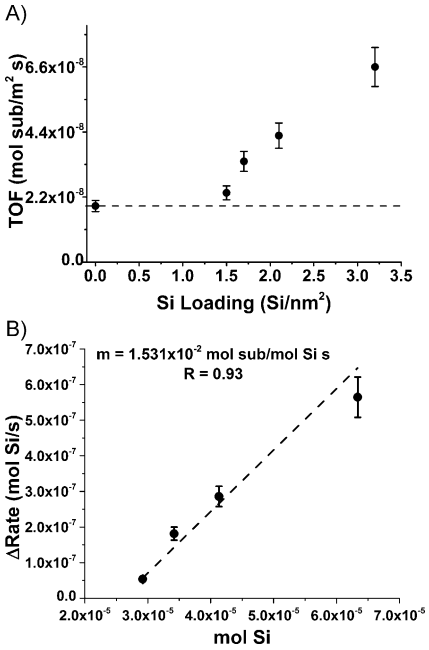

Figure 4. Cyclohexanol dehydration kinetics over SiO_x/Al_2O_3. A) Turnover frequencies for 0.0–3.2 Si/nm^2 SiO_x/Al_2O_3 catalysts. Units: mol substrate/(m^2 cat s). B) Rate difference per mol Si on SiO_x/Al_2O_3 catalysts. The rate of pure alumina is subtracted from the rate of each catalyst to approximate the specific activity of the Si sites, expressed as the slope m of the linear regression. Units: mol substrate/(mol Si s).

Note that the present SiO_x/Al_2O_3 catalysts provide higher initial turnover frequencies (normalized to catalyst surface area, Figure 4A) versus the parent γ-Al_2O_3. The SiO_x/Al_2O_3 TOF reaches a maximum of 6.6×10^{-8} mol substrate/(m^2 cat s) at the highest Si loading, a 3.5-fold increase over that of γ-Al_2O_3, 1.9×10^{-8} mol substrate/(m^2 cat s). SiO_2 was found to be catalytically inert under the same conditions, differentiating the Brønsted acidity of the isolated SiO_x site from polymeric SiO_2. A commercially available 6.5 wt % SiO_2–Al_2O_3 catalyst was screened for comparison. While the TOF of the commercial catalyst (1.4×10^{-7} mol substrate/(m^2 cat s)) was found to be 2 times that of our highest TOF (6.6×10^{-8} mol substrate/(m^2 cat s)), the carbon balance of the reaction was only 68 %, indicating significant carbon loss consistent with heavy product formation (Figure S22). We hypothesize that this difference in carbon balance is a result of the milder acidity of the SiO_x species relative to strong Brønsted sites in conventional SiO_2–Al_2O_3 and demonstrates the value of tuning the strength and homogeneity of solid acid catalysts.

Since the DNP-enhanced CPMAS NMR and infrared spectroscopies indicate (see above) that the SiO_x/Al_2O_3 alumina character is largely unchanged after calcination, it is reasonable to assume the parent alumina catalytic activity remains approximately constant at all Si loadings. This allows for subtraction of the alumina rate contribution from the apparent SiO_x/Al_2O_3 rates (Figure 4B). The resulting linear increase in rate per mol Si strongly argues that all surface Si sites are uniformly active in the cyclohexanol dehydration, and the slope of the linear regression yields a turnover frequency per Si site of 1.5×10^{-2} mol substrate/(mol Si s).

As a further comparison, a surface-acid SiO_2/Al_2O_3 catalyst was prepared according to the wet chemical CLD technique of van Bokhoven.[11b] This catalyst was selected because it represents an umambiguous, direct comparison to our own, being prepared from the same precursors, TEOS and γ-Al_2O_3, but under different synthetic conditions. In addition, the physical and acidic properties of such catalysts have been extensively characterized.[7b,11] The catalyst was prepared with a single Si deposition reaction using an γ-Al_2O_3 identical to that in the ALD syntheses (further description in Figure S9). The liquid-phase technique yields a catalyst of substantially similar surface area ($56\ m^2g^{-1}$), particle size ($< 3\ \mu m$), and Si content (2.8 Si/nm^2). However, the catalytic results (Figures S22 and S23) deviate from those observed with the ALD-derived catalysts. Analysis of catalytic activity and selectivity is hampered by apparent leaching of Si from the catalyst under reaction conditions, as Si-containing species are observed by GC-MS and ^{29}Si NMR (principally cyclohexyl ethers of Si). Selectivity to cyclohexene is low ($< 20\%$), and other products, including dicyclohexyl ether and cyclohexylcyclohexane, are observed. Despite the leaching, catalytic activity comparable to SiO_x/Al_2O_3 catalysts on a surface area basis (4.7×10^{-8} mol substrate/(m^2 cat s)) was observed, but based on the catalyst Si content, the Si sites do not show the same activity as those in SiO_x/Al_2O_3 ($< 1.5 \times 10^2$ mol substrate/(mol Si s)). The origin of this difference is at present unclear and promises a rich question for future study. In addition some structural differences in previously prepared CLD catalysts are noted, as characterized by FTIR[11a] and DNP-enhanced CPMAS SSNMR.[11c]

In summary, we report the synthesis of a novel class of highly dispersed SiO_x/Al_2O_3 catalysts by the vapor-phase reaction of TEOS with γ-Al_2O_3. Significant surface Brønsted acidity is observed that tracks the Si coverage in a linear fashion, implying along with XPS, NMR, and DRIFTS spectroscopic data, an $(\text{-AlO})_3\text{Si(OH)}$ active site assignment. The silanol proton is catalytically competent, and the SiO_x/Al_2O_3 sites exhibit higher catalytic activity than γ-Al_2O_3 sites in cyclohexanol dehydration. In contrast to stronger Brønsted acid sites in a conventional silica–alumina catalyst, no carbon loss is detected, demonstrating the attraction of more uniform/less acidic SiO_x sites.

Acknowledgements

Financial support from the NSF (CHE-1213235), IACT (DE-AC02-06CH11357), and ICEP (DE-FG02-03ER15457) is gratefully acknowledged. GC-TOF instrumentation at the Integrated Molecular Structure and Research Center (IMSERC) was supported by the NSF (CHE-0923236). This work made use of the Epic Facility (NUANCE Center-Northwestern University), which has received support from the MRSEC program (NSF DMR-1121262) at the Materials Research Center, The Nanoscale Science and Engineering Center (EEC-0118025/003), both programs of the National Science Foundation; the State of Illinois; and Northwestern University. The Clean Catalysis Facility of the Northwestern University Center for Catalysis and Surface Science is supported by a grant from the DOE (DE-SC0001329). Solid-state NMR studies at Ames Laboratory were supported by the U.S. DOE, Office of Basic Energy Sciences, Division of Chemical Sciences, Geosciences, and Biosciences through the Ames Laboratory under Contract No. DE-AC02-07CH11358. We thank A. Weingarten for helpful contributions.

Keywords: alcohol dehydration · atomic layer deposition · heterogeneous catalysis · silica-alumina · solid acid

[1] K. Tanabe, in *Solid Acids and Bases* (Ed.: K. Tanabe), Academic Press, San Diego, **1970**, pp. 1–3.
[2] a) C. L. Thomas, *Ind. Eng. Chem.* **1949**, *41*, 2564–2573; b) B. E. Yoldas, *J. Non-Cryst. Solids* **1984**, *63*, 145–154; c) N. Yao, G. Xiong, M. He, S. Sheng, W. Yang, X. Bao, *Chem. Mater.* **2002**, *14*, 122–129.
[3] a) C. J. Plank, E. J. Rosinski, W. P. Hawthorne, *I&EC Prod. Res. Dev.* **1964**, *3*, 165–169; b) E. G. Derouane, J. C. Védrine, R. R. Pinto, P. M. Borges, L. Costa, M. A. N. D. A. Lemos, F. Lemos, F. R. Ribeiro, *Catal. Rev.* **2013**, *55*, 454–515.
[4] a) F. F. Roca, L. De Mourgues, Y. Trambouze, *J. Catal.* **1969**, *14*, 107–113; b) M. Guisnet, N. S. Gnep, S. Morin, *Microporous Mesoporous Mater.* **2000**, *35–36*, 47–59.
[5] a) J. H. Lunsford, *Catal. Today* **2000**, *63*, 165–174; b) D. Chen, K. Moljord, A. Holmen, *Microporous Mesoporous Mater.* **2012**, *164*, 239–250.
[6] H. Kawakami, S. Yoshida, T. Yonezawa, *J. Chem. Soc. Faraday Trans. 2* **1984**, *80*, 205–217.
[7] a) D. G. Poduval, J. A. R. van Veen, M. S. Rigutto, E. J. M. Hensen, *Chem. Commun.* **2010**, *46*, 3466–3468; b) M. Caillot, A. Chaumonnot, M. Digne, J. A. van Bokhoven, *J. Catal.* **2014**, *316*, 47–56.
[8] a) M. Trombetta, G. Busca, S. Rossini, V. Piccoli, U. Cornaro, A. Guercio, R. Catani, R. J. Willey, *J. Catal.* **1998**, *179*, 581–596; b) W. Suprun, M. Lutecki, T. Haber, H. Papp, *J. Mol. Catal. A* **2009**, *309*, 71–78.
[9] a) G. P. Heitmann, G. Dahlhoff, W. F. Hölderich, *J. Catal.* **1999**, *186*, 12–19; b) R. Martinez, M. C. Huff, M. A. Barteau, *Appl. Catal. A* **2000**, *200*, 79–88.
[10] a) O. M. Gazit, A. Katz, *Langmuir* **2012**, *28*, 431–437; b) O. M. Gazit, A. Katz, *J. Am. Chem. Soc.* **2013**, *135*, 4398–4402.
[11] a) M. Caillot, A. Chaumonnot, M. Digne, J. A. V. Bokhoven, *ChemCatChem* **2013**, *5*, 3644–3656; b) M. Caillot, A. Chaumonnot, M. Digne, C. Poleunis, D. P. Debecker, J. A. van Bokhoven, *Microporous Mesoporous Mater.* **2014**, *185*, 179–189; c) M. Valla, A. J. Rossini, M. Caillot, C. Chizallet, P. Raybaud, M. Digne, A. Chaumonnot, A. Lesage, L. Emsley, J. A. van Bokhoven, C. Copéret, *J. Am. Chem. Soc.* **2015**.

[12] J. Datka, B. Gil, O. Vog, J. Rakoczy in *Stud. Surf. Sci. Catal.*, *Vol. 125* (Eds.: I. Kiricsi, G. Pál-Borbély, J. B. Nagy, H. G. Karge), Elsevier, Amsterdam **1999**, pp. 409 – 415.
[13] J. He, C. Zhao, J. A. Lercher, *J. Catal.* **2014**, *309*, 362 – 375.
[14] a) M. Niwa, S. Kato, T. Hattori, Y. Murakami, *J. Chem. Soc. Faraday Trans. 1* **1984**, *80*, 3135 – 3145; b) S. Sato, M. Toita, Y.-Q. Yu, T. Sodesawa, F. Nozaki, *Chem. Lett.* **1987**, *16*, 1535 – 1536.
[15] J. W. Klaus, S. M. George, *Surf. Sci.* **2000**, *447*, 81 – 90.
[16] J. D. Ferguson, E. R. Smith, A. W. Weimer, S. M. George, *J. Electrochem. Soc.* **2004**, *151*, G528 – G535.
[17] Z. Ma, S. Brown, J. Y. Howe, S. H. Overbury, S. Dai, *J. Phys. Chem. C* **2008**, *112*, 9448 – 9457.
[18] J. W. Elam, M. D. Groner, S. M. George, *Rev. Sci. Instrum.* **2002**, *73*, 2981 – 2987.
[19] R. L. Puurunen, *J. Appl. Phys.* **2005**, *97*, 121301.
[20] A. F. Lee, D. E. Gawthrope, N. J. Hart, K. Wilson, *Surf. Sci.* **2004**, *548*, 200 – 208.
[21] a) E. Paparazzo, *Surf. Interface Anal.* **1988**, *12*, 115 – 118; b) L. Galán, I. Montero, F. Rueda, J. M. Albella, *Surf. Interface Anal.* **1992**, *19*, 473 – 477.
[22] a) T. L. Barr, *Zeolites* **1990**, *10*, 760 – 765; b) I. Böszörményi, T. Nakayama, B. McIntyre, G. Somorjai, *Catal. Lett.* **1991**, *10*, 343 – 355.
[23] a) T. Maly, G. T. Debelouchina, V. S. Bajaj, K.-N. Hu, C.-G. Joo, M. L. Mak-Jurkauskas, J. R. Sirigiri, P. C. A. van der Wel, J. Herzfeld, R. J. Temkin, R. G. Griffin, *J. Chem. Phys.* **2008**, *128*, 052211 – 052219; b) A. Lesage, M. Lelli, D. Gajan, M. A. Caporini, V. Vitzthum, P. Miéville, J. Alauzun, A. Roussey, C. Thieuleux, A. Mehdi, G. Bodenhausen, C. Coperet, L. Emsley, *J. Am. Chem. Soc.* **2010**, *132*, 15459 – 15461.
[24] G. Engelhardt, D. Michel, *High-Resolution Solid-State NMR of Silicates and Zeolites*, Wiley, Chichester, **1987**.
[25] a) M. McMillan, J. S. Brinen, J. D. Carruthers, G. L. Haller, *Colloids and Surfaces* **1989**, *38*, 133 – 148; b) N. Katada, M. Niwa, *Res. Chem. Intermed.* **1998**, *24*, 481 – 494.
[26] M. Casarin, D. Falcomer, A. Glisenti, M. M. Natile, F. Poli, A. Vittadini, *Chem. Phys. Lett.* **2005**, *405*, 459 – 464.
[27] a) G. Busca, *Catal. Today* **2014**, *226*, 2 – 13; b) E. Finocchio, G. Busca, S. Rossini, U. Cornaro, V. Piccoli, R. Miglio, *Catal. Today* **1997**, *33*, 335 – 352.
[28] T. C. Sheng, S. Lang, B. A. Morrow, I. D. Gay, *J. Catal.* **1994**, *148*, 341 – 347.
[29] a) J. B. Peri, R. B. Hannan, *J. Phys. Chem.* **1960**, *64*, 1526 – 1530; b) M. Niwa, N. Katada, Y. Murakami, *J. Phys. Chem.* **1990**, *94*, 6441 – 6445.
[30] M. R. Basila, T. R. Kantner, *J. Phys. Chem.* **1967**, *71*, 467 – 472.
[31] D. P. Sobczyk, J. J. G. Hesen, J. van Grondelle, D. Schuring, A. M. de Jong, R. A. van Santen, *Catal. Lett.* **2004**, *94*, 37 – 43.
[32] K. I. Hadjiivanov, G. N. Vayssilov in *Advances in Catalysis*, *Vol. 47*, Academic Press, San Diego, **2002**, pp. 307 – 511.
[33] a) L. Oliviero, A. Vimont, J.-C. Lavalley, F. Romero Sarria, M. Gaillard, F. Mauge, *Phys. Chem. Chem. Phys.* **2005**, *7*, 1861 – 1869; b) K. Hadjiivanov in *Advances in Catalysis*, *Vol. 57* (Ed.: C. J. Friederike), Academic Press, San Diego **2014**, pp. 99 – 318.
[34] F. Garcia-Ochoa, A. Santos, *Ind. Eng. Chem. Res.* **1993**, *32*, 2626 – 2632.

Received: June 13, 2015
Revised: August 31, 2015
Published online: ■■ ■■, ■■■■

Communications

Heterogeneous Catalysis

A. R. Mouat, C. George, T. Kobayashi, M. Pruski, R. P. van Duyne, T. J. Marks,* P. C. Stair* _____ ■■■■–■■■■

Highly Dispersed SiO_x/Al_2O_3 Catalysts Illuminate the Reactivity of Isolated Silanol Sites

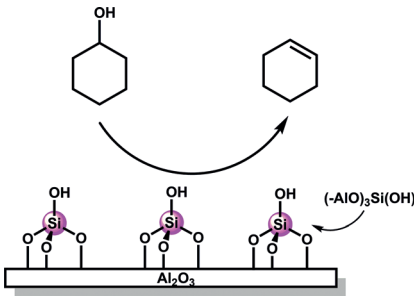

Strong enough to get the job done: By selectively installing isolated $(\text{-AlO})_3\text{SiOH}$ species on a $\gamma\text{-}Al_2O_3$ substrate, a unique "mild" Brønsted-acid catalytic site is formed. These well-defined sites evince highly uniform characteristics and are catalytically competent in the dehydration of cychohexanol, showing higher activity, no loss of selectivity, and no coking.